Metal−Metal Bonding and Metallic Behavior in Some ABO_2 Delafossites

R. Seshadri, C. Felser, K. Thieme, and W. Tremel*

Institut für Anorganische Chemie und Analytische Chemie, Johannes Gutenberg-Universität, Mainz, Becher Weg 24, D55099, Mainz, Germany

Received February 10, 1998. Revised Manuscript Received April 29, 1998

We present results of ab initio band structure calculations on some ABO_2 delafossite oxides that have both the A and B sites occupied by transition metals. This class of materials includes insulators as well as some of the most conducting oxides. The calculations have been performed in order to understand the nature of the metallic and insulating states and the extensive metal−metal bonding displayed by these materials. The effect of polytypism on the electronic structure is examined. Among the interesting aspects of the electronic structure of these materials are the contributions from both A and B atoms to states near the Fermi energy and the highly disperse nature of bands derived from the d_{z^2} orbitals of the A atom. This last feature is expected to be important for stabilizing metallic ground states.

Introduction

The ABO_2 delafossites[1] comprise layers of edge-connected BO_2 octahedra with the $Cd(OH)_2$ structure[2] tethered to one another through two-coordinate A atoms. The archetype is the mineral $CuFeO_2$ (delafossite) which has two-coordinate Cu^I in the A site tethering layers of $Fe^{III}O_2$ octahedra.[3,4] An alternate description of the structure considers close-packed CuO_2 rods with the octahedral sites between O occupied by Fe. A key feature of this structure type is that both the A as well as the B atoms form triangular arrays. The two-coordinate, low valent A site is a feature worthy of note in this structure. However, each A atom has six proximal A atoms in the plane as neighbors. This then suggests a third, rather unusual description of the structure as close-packed sheets (fcc 111) of the A metal atoms alternately stacked with BO_2 layers possessing the $Cd(OH)_2$ structure. The BO_2 sublattice (and the A sublattice) can show stacking variants so that the delafossites crystallize as hexagonal 2H structures, rhombohedral 3R structures, etc.

From the electronic structure viewpoint, two classes of delafossite materials may be identified. In the one, both A and B ions are transition metals. This class has been extensively studied by Shannon, Prewitt, and their co-workers[5−7] and includes ABO_2 with A = Cu, Pd, Ag, Pt; B = Sc, Cr, Fe, Co, and Rh. These workers noted particularly that while linear coordination is well-known for Cu^I and Ag^I, Pd and Pt are rarely observed in a formal monovalent state. They also noted that when A was Pd or Pt, the oxides were conducting (the in-plane conductivity of $PtCoO_2$ is on the order of $10^6\ \Omega^{-1}\ cm^{-1}$, only slightly smaller than Cu metal), but the compositions with the d^{10} cations, A = Ag and Cu, were insulating. This then led them to propose a tentative bonding scheme involving broad A cation d levels at the Fermi energy. More recently, Hagenmuller and co-workers established that $AgNiO_2$ is metallic[8] and that one obtains a compositionally controlled metal−semiconductor transition with increasing x in the series $AgNi_{1-x}Co_xO_2$.[9] Their interpretation of the metallic behavior is in terms of overlap between Ag and Ni d levels, which they claim is missing in the Co compounds.

The other class of delafossites have only one transition metal ion, the other cation being a highly ionized trivalent species that is relatively inert from the perspective of electrical properties, not being able to contribute to states at or near the Fermi energy. This class is exemplified by $CuLnO_2$ (Ln is Y or a rare-earth), which has attracted recent interest since it provides triangular Cu lattices for comparison with the square nets of Cu found in the copper oxide superconductors. The delafossites are of considerable interest from a magnetic viewpoint because of the intrinsic frustration of bond antiferromagnetism in triangular lattices. There is now additional impetus for studying these systems because suggestions by Rice and co-workers[10] that certain spin ladder systems can be doped to supercon-

(1) Wells, A. F. *Structural Inorganic Chemistry*, 5th ed.; Clarendon Press: Oxford, 1984.
(2) More commonly referred to as the CdI_2 structure type. See: Hyde, B. G.; Andersson, S. *Inorganic Crystal Structures;* John Wiley: New York, 1989.
(3) Soller, W.; Thompson, A. J. *Phys. Rev.* **1935**, *47*, 644.
(4) Pabst, A. *Am. Mineral.* **1946**, *31*, 539.
(5) Shannon, R. D.; Rogers D. B.; Prewitt, C. T. *Inorg. Chem.* **1971**, *10*, 713.
(6) Prewitt, C. T.; Shannon, R. D.; Rogers, D. B. *Inorg. Chem.* **1971**, *10*, 719.
(7) Rogers, D. B.; Shannon, R. D.; Prewitt, C. T.; Gillson, J. L. *Inorg. Chem.* **1971**, *10*, 723.
(8) Wichainchai, A.; Dordor, P.; Doumerc, J. P.; Marquestaut, E.; Pouchard, M.; Hagenmuller, P.; Ammar, A. *J. Solid State Chem.* **1988**, *74*, 126.
(9) Shin, Y. J.; Doumerc, J. P.; Dordor, P.; Pouchard, M.; Hagenmuller, P. *J. Solid State Chem.* **1993**, *107*, 194.
(10) Rice, T. M.; Gopalan, S.; Sigrist, M. *Europhys. Lett.* **1993**, *23*, 445.

S0897-4756(98)00079-9 CCC: $15.00
Published on Web 07/25/1998

Table 1. Crystal Structures of the 3R Delafossites and 2H $AgFeO_2$

compound	*a* (Å)	*c* (Å)	O *z*/*c*[b]	BVS A site	BVS B site	trig comp[c]	ref
			3R Delafossites[a]				
$AgFeO_2$	3.0391	18.590	0.1112	1.092	2.838	0.892	6
$AgCoO_2$	2.8750	18.374	0.1144	0.990	3.156	0.883	9
$AgNiO_2$	2.9400	18.360	0.1143	1.000	2.557	0.872	9
$PdCoO_2$	2.8300	17.743	0.1112	0.868	3.246	0.904	6
$PtCoO_2$	2.8300	17.834	0.1140	1.066	3.456	0.890	6
			2H $AgFeO_2$[d]				
	3.0390	12.395	0.0833	1.088	2.644	0.892	17

[a] Space group $R\bar{3}m$. A in (0, 0, 0); B in (0, 0, $^1/_2$); O in (0, 0, *z*). [b] For 3R $AgCoO_2$ and 3R $AgNiO_2$, this was fixed through the BVS as explained in the text. [c] Compression of the BO_6 octahedra down the *c* axis defined as d_{O-O}(apical)/d_{O-O}(in plane). [d] Space group $P6_3/mmc$. A in ($^1/_3$, $^2/_3$, $^1/_4$); B in (0, 0, 0); O in ($^1/_3$, $^2/_3$, *z*)

ductivity have been realized experimentally.[11] Spin ladders with an even number of "legs" show spin frustration, as do the delafossites. Oxygen doping in 2H $CuYO_2$ and 3R $CuLaO_2$ has been studied,[12] as have the electronic structures of pristine and oxygen-doped 2H $CuYO_2$.[13] Recently, the possible use of $CuAlO_2$ as a transparent ionic conductor has been pointed out.[14] This compound would also fall into this second class of delafossites.

In this contribution, we examine the electronic structure of delafossites from the first class described above, focusing on 3R ABO_2. The scheme is as follows: We study the effect of going across the late first row transition metals at the B site (B = Fe, Co and Ni) for $AgBO_2$. Then with B = Co, we follow the influence of changing A from Ag to Pd and Pt. To see whether there is any influence of the stacking variant on the electronic structure, we compare the densities of state (DOS) of 2H $AgFeO_2$ and 3R $AgFeO_2$. The band structures of specific delafossites are then examined. The calculations have been carried out by employing the tight-binding linearized muffin-tin orbital method using the atomic sphere approximation (TB-LMTO-ASA) level within the local (spin) density approximation [L(S)DA]. The main intention has been to examine whether the observed metallic or insulating behavior can be reproduced within the LDA and, in the case of the metallic compounds, to determine which atoms contribute to states at E_F. We also speculate on the importance of electron correlation in these systems and what effect the neglect of possible antiferromagnetism (enforced because of the spin frustration) can have on the LDA energy levels.

A chemically interesting feature in these structures are the extremely short A−A and B−B contacts, equal to the *a* lattice parameter. As an example, in 3R $AgCoO_2$, the Ag−Ag distance is 2.875 Å,[5] compared to silver metal where it is 2.889 Å.[15] Despite such short metal−metal contact, this compound is insulating. It is thus of interest to examine in some detail the nature of the bonds formed between the A atoms in these delafossites. To this end, we present an analysis of the crystal orbital Hamiltonian populations (COHP), a recently developed tool for the analysis of specific bonding between atoms.

Methods

Crystal Structures. Table 1 lists the structures of the 3R compounds $AgFeO_2$, $AgCoO_2$, $AgNiO_2$, $PdCoO_2$, and $PtCoO_2$. The structures of 3R $AgFeO_2$, 3R $PdCoO_2$, and 3R $PtCoO_2$ were taken from ref 6 The lattice parameters for 3R $AgCoO_2$ and 3R $AgNiO_2$ were taken from ref 9. The oxygen *z* positions for the last two were calculated using the bond-valence program valence[16] in order that Ag had a bond valence sum of unity. The structure of 2H $AgFeO_2$ was taken from the work of Okamoto et al.[17] and is also presented in Table 1. Views of the 2H and 3R structures of $AgFeO_2$ using crystal coordinates are presented in panels a and b of Figure 1. The view is almost looking down *b*. Panel c of this figure shows the octahedral arrangement of oxygen around the B site. The view is down the 3- or 6-fold *c* axis. The bond valence sums of the atoms in the two sites for the different compounds confirm that the crystal structures are consistent with the presence of trivalent B cations and monovalent A cations, even though the latter is unusual for Pd and Pt, as pointed out originally by Shannon et al.[5] There seem to be no systematic changes either in bond valence or in the trigonal compression (squashing) of the BO_6 octahedra that might be indicative of the electronic states (transitions from metallic to insulating behavior, etc.).

The Experimental Situation. Of the compounds studied here, $AgNiO_2$,[8] $PdCoO_2$, and $PtCoO_2$[7] are metallic. $AgCoO_2$[7,9] and 3R $AgFeO_2$[7] are insulating. While the transport properties of 2H $AgFeO_2$[17] have not been reported, the red color of the crystals suggests insulating behavior. The magnetic properties of $AgNiO_2$[8] correspond to low-spin Ni^{3+}. $AgCoO_2$[9] shows weak paramagnetism, in keeping with low-spin Co^{3+}, the paramagnetic contribution arising either from trace impurities or from a slight high-spin component. We recollect that Co^{3+} in $LaCoO_3$ undergoes spin-state transitions.[18] Likewise, $PdCoO_2$ is reported to have low-spin diamagnetic Co^{3+}, with negligible contribution to the susceptibility from d^9 Pd^+ due to delocalization.[7] This is also true for $PtCoO_2$. To our knowledge, the magnetic properties of the Fe compounds have not been reported.

Calculation Details and Reciprocal Space. The central Brillouin zone of the rhombohedral 3R ABO_2 delafossites follows standard labeling. The high symmetry points are Γ(0, 0, 0), *Z*(0, 0, $^a/_{2c}$), *F*($^1/_6$, $^1/_3$, $^a/_{3c}$), and *L*($-^1/_6$, $^1/_3$, $^a/_{6c}$) in units of $^{2\pi}/_a$. In terms of the reciprocal basis vectors, the coordinates are Γ(0, 0, 0), *Z*($^1/_2$, $^1/_2$, $^1/_2$), *F*($^1/_2$, $^1/_2$, 0), and *L*(0, $^1/_2$, 0) as described in ref 19.

(11) Uehara, M.; Nagata, J.; Akimitsu, J.; Takahashi, H.; Mori, N.; Kinoshita, K. *J. Phys. Soc. Jpn.* **1996**, *65*, 2764.
(12) Cava, R. J.; Zandbergen, H. W.; Ramirez, A. P.; Takagi, H.; Chen, C. T.; Krajewski, J. J.; Peck Jr., W. F.; Waszczak, J. V.; Meigs, G.; Roth, R. S.; Schneemeyer, L. F. *J. Solid State Chem.* **1993**, *104*, 437.
(13) Mattheiss, L. F. *Phys. Rev. B.* **1993**, *48*, 18300.
(14) Kawazoe, H.; Yasukawa, M.; Hyodo, H.; Kurita, M.; Yanagi, H.; Hosono, H. *Nature* **1997**, *389*, 938.
(15) Donohue, J. *The Structure of the Elements;* John Wiley: New York, 1974.
(16) Hormillosa, C.; Healy, S.; Computer code valence, McMaster University, Hamilton, Canada, 1991; Brown, I. D.; Altermatt, D. *Acta Crystallogr. B* **1995**, *41*, 244.
(17) Okamoto, S.; Okamoto, I.; Ito, T. *Acta Crystallogr. B* **1972**, *28*, 1774.
(18) Raccah, P. M.; Goodenough, J. B. *Phys. Rev.* **1967**, *155*, 932.

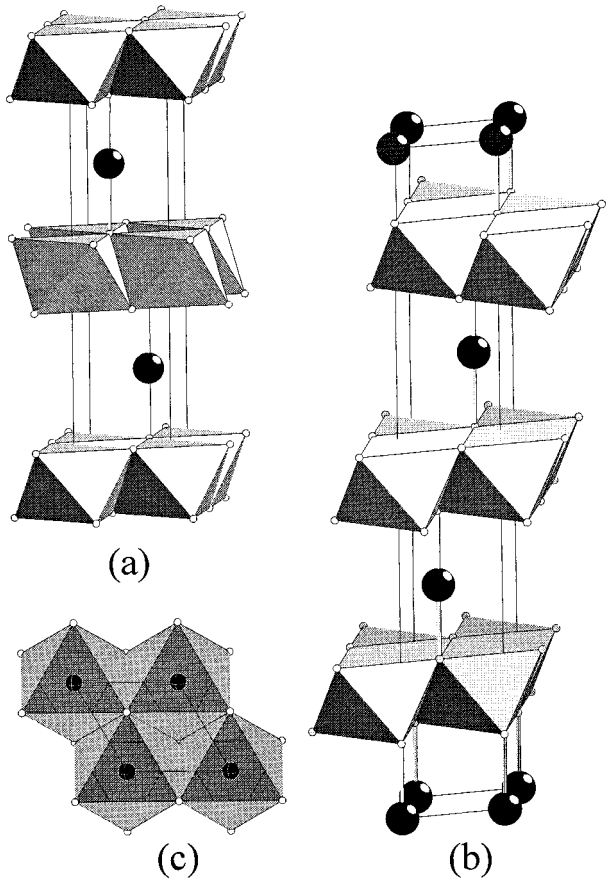

Figure 1. (a) Structure of 2H $AgFeO_2$, showing the two-coordinate Ag and the FeO_6 octahedra. The view is down the *b* axis. (b) View down the *b* axis of 3R $AgFeO_2$. (c) View of the delafossite structure looking down the *c* axis.

The electronic structures presented here were calculated using the self-consistent, scalar relativistic linearized muffin-tin orbital (LMTO) program of Andersen et al.[20,21] within the atomic sphere approximation (ASA). The exchange-correlation potential of the density functional theory (DFT) is obtained within the local density approximation (LDA) using the method of von Barth and Hedin.[22] The LMTO method is described in detail elsewhere[21,23] and only some key points are mentioned here. *k* space integrations employed the tetrahedron method using more than 300 irreducible *k* points within the Brillouin zone. The basis sets consisted of the valence s, p, and d orbitals of the transition metals and the 2p orbitals of oxygen. The 2s orbital of oxygen and the f orbitals of Pd, Ag, and Pt were dealt with using the downfolding technique. Special care was taken in filling the interatomic space in the structure with empty spheres, the sphere radii and the positions of which are chosen in such a way that space filling is achieved without exceeding a sphere overlap of 16%. This was done using an automatic procedure developed by Krier et al.[24] Figure 2 illustrates the use of empty spheres for the example of 3R $AgFeO_2$, and Table 2 lists, as illustrative for all the compounds, the positions and radii of the atomic and empty spheres used for calculating the electronic structure of this compound. The empty spheres are treated in the calculations using s-like muffin-tin orbitals without cores. It was verified that the results presented here were not changed on increasing the number of irreducible *k* points. The results were also not greatly affected by small changes (made by hand) in the *z* parameter of oxygen, which is the only free structural parameter (apart from the lattice parameters). However, using the ASA, structural changes that are not isotropic do not yield changes in the total energy that can be reliably compared or used for determining minima.

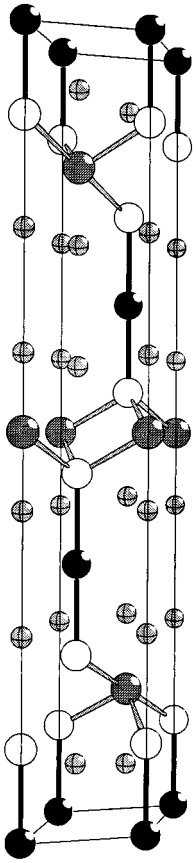

Figure 2. Structure of 3R $AgNiO_2$, showing the Ag (black, closed), Ni (gray, closed), and O (white) atoms and their connectivity, as well as the empty spheres (gray, crossed) used in the LMTO calculations. The view is a perspective almost down the *b* axis. The radii depicted are not to scale.

Table 2. Radii and Positions of the Atomic and Empty Spheres in 3R $AgNiO_2$

sphere	radius (Å)	*x*/*a*	*y*/*b*	*z*/*c*
Ag	1.5434	0	0	0
Ni	1.2243	0	0	0.5
O	0.9910	0	0	0.1143
E1	1.0670	0	0	0.25
E2	0.8065	0	0	0.4028

To elaborate the nature of bonding between atoms, we utilize two relatively recent tools in the TB-LMTO program package of Andersen et al. Decorating bands with a width (chosen usually as 2.5% of the total energy scale for convenient visualization) proportional to the sum of the weights of the corresponding orthonormal orbitals obtains "fatbands" that reveal the orbital character of bands.[25] The bonding is revealed through the use of the crystal orbital Hamiltonian populations (COHPs) that as a function of energy can be negative and antibonding, zero and nonbonding, and positive, implying bonding.[26] The COHPs are the densities of state weighted by the corresponding Hamiltonian matrix element.

(19) Bradley, C. J.; Cracknell, A. P. *The Mathematical theory of symmetry in solids;* Clarendon Press: Oxford, 1972.
(20) Andersen, O. K.; Jepsen, O.; et al. TB-LMTO-ASA47, MPI für Festkörperforschung, Stuttgart, Germany, 1996.
(21) Andersen, O. K.; Jepsen, O.; Snob, M. *Linearized Band-Structure Methods in Electronic Band-Structure and its Applications;* Springer Lecture Notes in Physics, 1987.
(22) von Barth, U.; Hedin, L. *J. Phys. C* **1972**, *4*, 2064.
(23) Skriver, H. L. *The LMTO method;* Springer: Berlin, 1984.
(24) Krier, G.; Jepsen, O.; Andersen, O. K. Unpublished results.
(25) Jepsen, O.; Andersen, O. K. *Z. Phys. B* **1995**, *97*, 35.
(26) Boucher, F.; Jepsen, O.; Andersen, O. K. Unpublished results; Boucher, F.; Rousseau, R. *Inorg. Chem.* **1998**, *37*, 2351.

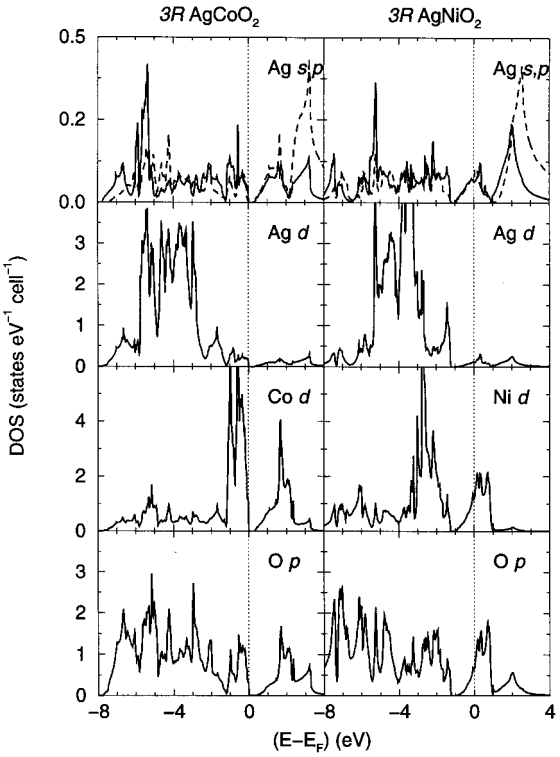

Figure 3. Orbital-projected densities of state for 3R $AgCoO_2$ and $AgNiO_2$. The orbitals that contribute to the DOS are labeled. The DOS due to Ag p orbitals are depicted using broken lines.

The COHPs are similar to the crystal orbital overlap populations (COOPs) introduced by Hoffmann and co-workers,[27] except that the sign convention is the opposite of the one used here (negative is bonding, etc.) and the DOS is weighted by the overlap. COHPs have been used previously in refs 28 and 29. A separate implementation of COHPs has been given in ref 30, but with the opposite sign convention being used.

For all the compounds, spin-polarized calculations were carried out. It appears that only the Fe compounds have a finite magnetization within the LSDA, so it is only for this compound that the results of the spin-polarized calculation are presented.

Results and Discussion

Densities of State. We commence by considering the orbital-projected densities of state (DOS) across the series 3R $AgBO_2$ with B = Co and Ni. These DOS are displayed in the eight panels of Figure 3 and depict, for the two compounds, the DOS due to silver s and p (broken lines) states, the silver d states, the B atom d states, and oxygen p states.

Considering the formulation $Ag^{+}Co^{3+}O_2^{2-}$, we expect a fully occupied Ag d band, empty Ag s and (for low-spin Co^{3+}) a filled t_{2g} Co band. We see, as expected from Figure 3, that the s and p orbital derived states of Ag are broad, while the d states are less so. The bandwidths of the Ag d states are similar for the Ni and Co compounds.

The states due to the d orbitals of Co and Ni in the two compounds are separated by a gap between t_{2g} and e_g corresponding to a low-spin arrangement, the separation being nearly constant (~0.5 eV) for the two compounds. The d states display a nearly rigid band behavior, the gross features being similar across the series Co and Ni. The only change is the electron count which results in (within the LDA) the Co compound being a band insulator and the Ni compound being metallic with electrons as carriers. The states due to metallic Ni t_{2g} are slightly broader than the Co t_{2g} derived states, the widths respectively being about 2 and 1.2 eV. Most of states derived from oxygen p orbitals occur over a large energy range, spanning −8 to −2 eV. There are oxygen states also in the same energy region as the B atom d states due to strong metal−ligand mixing. Considering the contribution from oxygen to the states at E_F, we notice an increase from Co to Ni. This is in keeping with experimentally observed trends in the optical spectra of the first row transition metal perovskites $LaMO_3$, where it is seen that metal d−oxygen p mixing near the gap increases as one traverses the 3d transition metals.[31] This could be the reason for the Ni t_{2g} states being more disperse. It is interesting to note that silver states are found at E_F only when the d states of the B atoms are also present.

To understand the effect of polytypism in this structure type on the bonding patterns, we compare 3R $AgFeO_2$ with 2H $AgFeO_2$. The spin-polarized calculations on the two Fe compounds 3R $AgFeO_2$ and 2H $AgFeO_2$ yield the result that both compounds have a calculated LSDA magnetic moment of 0.3 μ_B per Fe atom, which is one-third the spin-only value. Here, while the magnetic ground states correspond to ferromagnetism, the possibility of more complex behavior must be considered. The calculations were performed on the simple unit cell and no possibility of antiferromagnetic ordering was permitted, though antiferromagnetism is more in keeping with the insulating behavior. As mentioned earlier, the topological frustration of bond antiferromagnetism makes the construction of putative antiferromagnetic supercells difficult. An experimental system with which comparison might be drawn is $FeCl_3$, which has the $Cd(OH)_2$ structure with an ordered Fe vacancy and thus the same octahedral arrangement, as well as the same Fe oxidation state, as in the present system. $FeCl_3$ is weakly antiferromagnetic with a spiral magnetic structure due to competing interactions, the Néel temperature being 16 K.[32]

The eight panels of Figure 4 compare the spin-polarized, orbital-projected densities of state of the two Fe compounds. In each panel, the upper part corresponds to the majority spin states and the lower to the minority spin states. In the uppermost panels for both compounds, the Ag s and p states are presented. The latter are dotted. The densities of state of the compounds correspond to the primitive cell and hence for the 2H compound have been scaled to one formula unit through halving. As in the case of 3R $AgNiO_2$, the presence of Fe states at E_F result simultaneously in the presence of Ag states. Fe is low-spin, as expected for a d^5 system, and the E_F crosses the spin-minority t_{2g}

(27) Wijeyesekera, S.; Hoffmann, R. *Organometallics* **1984**, *3*, 949.
(28) Felser, C.; Deniard, P.; Bäcker, M.; Ohm, T.; Rouxel, J.; Simon, A. *J. Mater. Chem.* **1998**, *8*, 1295.
(29) Felser, C.; Finckh, E. W.; Kleinke, H.; Rocker, F.; Tremel, W. *J. Mater. Chem.* In press.
(30) Dronskowski, R.; Blochl, P. E. *J. Phys. Chem.* **1993**, *97*, 8617.
(31) Arima, T.; Tokura, Y.; Torrance, J. B. *Phys. Rev. B* **1993**, *48*, 17006.
(32) Cable, J. W.; Wilkinson, M. K.; Wollan, E. O. *Bull. Am. Phys. Soc.* **1960**, *5*, 458, as cited in Goodenough, J. B. *Magnetism and the Chemical Bond;* R. E. Krieger: Huntington, New York, 1976.

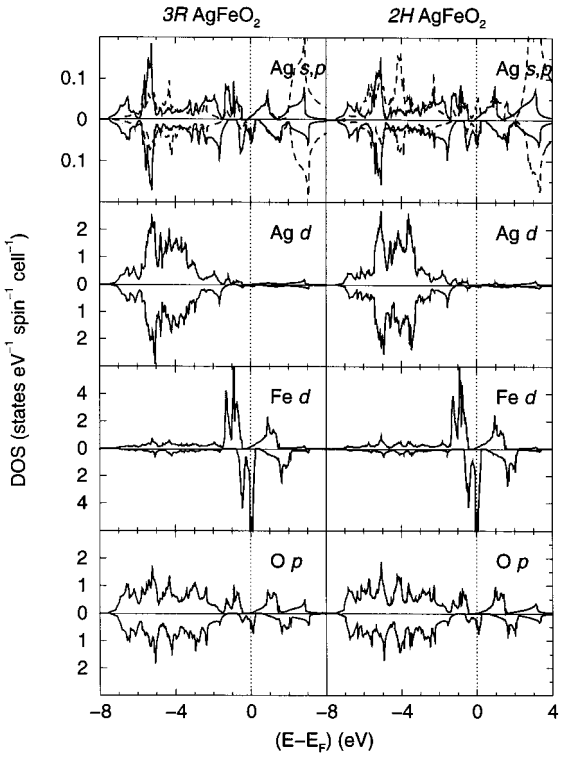

Figure 4. Orbital-projected densities of state for magnetic 3R $AgFeO_2$ and 2H $AgFeO_2$. In each panel, the majority and minority states are shown. The DOS due to Ag p orbitals are depicted using broken lines.

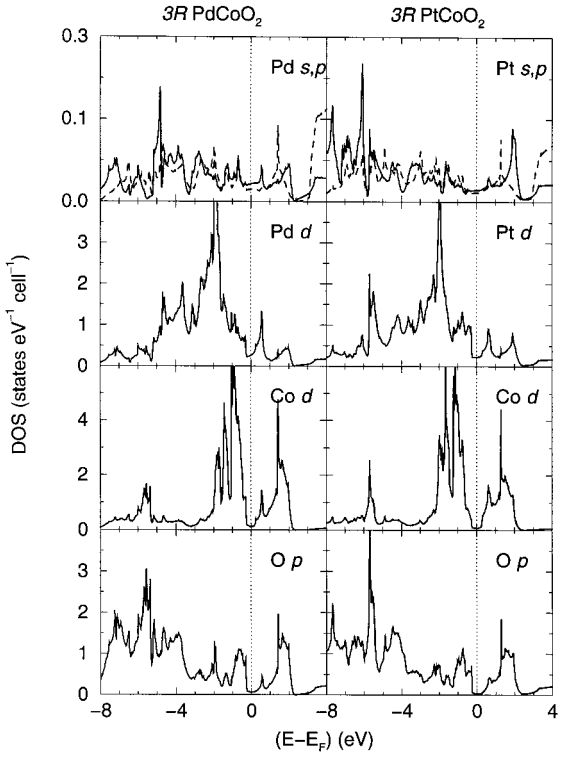

Figure 5. Orbital-projected densities of state for 3R $PdCoO_2$ and $PtCoO_2$. The orbitals that contribute to the DOS are labeled. The DOS due to Pd or Pt p orbitals are depicted using broken lines.

states in both polytypes, suggesting a metal with holes as carriers. The exchange splitting is small, in keeping with the small calculated magnetic moment. From an analysis of the t_{2g} fatbands, which are not shown here, we confirm that the spin polarization arises in the low-spin t_{2g} bands. The contribution at E_F due to O states is smallest in the Fe compounds, compared with the Co and Ni compounds. The spin polarization of the O and Ag states is negligible and arises due to polarization of Fe states. The gross features of the DOS support the view that polytypism does not greatly affect the electronic structure.

Within the LDA, $AgFeO_2$ and $AgNiO_2$ are metallic, with states at the Fermi energy, and $AgCoO_2$ is insulating with a band gap of around 0.5 eV. This result arises from the number of electrons in the unit cell; an odd number of electrons always give rise to states at E_F within the LDA, in the absence of magnetism. This is the case for the Fe and Ni compounds. However, the contrary is not true; systems with an even number of electrons *can* be metallic. The fact that $AgCoO_2$ is insulating thus suggests that it can be described as a band insulator, the gap being due to the separation of filled t_{2g} states of low-spin Co from empty e_g states. We now consider the nature of the metallic or insulating states. In the case of $AgFeO_2$, where experiment indicates insulating behavior, the LDA result seems to be incorrect. However, we note that the Fe d states are sharply peaked at E_F, resulting in a DOS that would imply an inherently unstable system. This is despite the spin polarization. Within the L(S)DA, we might speculate that a gap at the E_F can be opened through the formation of antiferromagnetic supercells that might have an even number of electrons within a unit cell in the sheet. The formation of an antiferromagnetic ground state with nearest-neighbor antiferromagnetic interactions is frustrated because of the triangular spin arrangement. That Fe t_{2g} states are rather narrow at E_F suggests that Coulomb correlations of the Hubbard U kind, which are ignored withing the L(S)DA, could make the $AgFeO_2$ delafossites insulating. Local rather than long-range magnetic correlations (as can be studied by diffuse neutron scattering and NMR) might play an important role to this end. By applying so-called Mott–Hubbard–Anderson models[33] that attempt to treat electron correlation as well as disorder within a single framework, it is known from applications to expanded metals[34] and to doped tungsten bronzes[35] that if the local coupling is antiferromagnetic (expected for Fe^{III} [36]), electrons will be localized, regardless of the degree of magnetic order or the state of doping. The result for 3R $AgNiO_2$ of a band metal with states at the Fermi energy mostly from the Ni–O pdσ* manifold, with a minor contribution from Ag states, seems reasonable and in keeping with the experimental situation,[8,9] with additional details discussed in the next section. One of the issues here is that Mott–Hubbard type correlations seem important for 3R $AgFeO_2$ but not for 3R $AgNiO_2$. This is in part because the states (in the LDA) at E_F are t_{2g} in the Fe compound and e_g in the Ni compound.

(33) Logan, D. E.; Szczech, Y. H.; Tusch, M. A. in Edwards, P. P.; Rao, C. N. R. (Eds.) *Metal–Insulator Transitions Revisited;* Taylor & Francis: London, 1995.
(34) Koslowski, T.; Rowan, D. G.; Logan, D. E. *Ber. Bunsen-Ges. Phys. Chem.* **1996**, *100*, 101.
(35) Dücker, H.; Koslowski, T.; von Niessen, W.; Tusch, M. A.; Logan, D. E. *J. Non-Crystalline Solids* **1996**, *205–207*, 32.
(36) Goodenough, J. B. *Magnetism and the Chemical Bond;* R. E. Krieger: Huntington, New York, 1976.

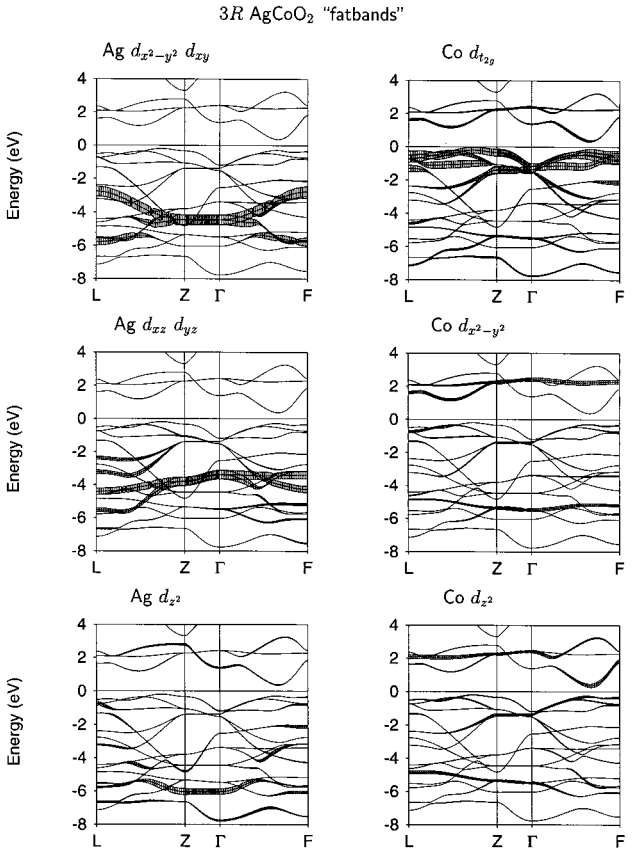

Figure 6. Selected fatbands of 3R $AgCoO_2$.

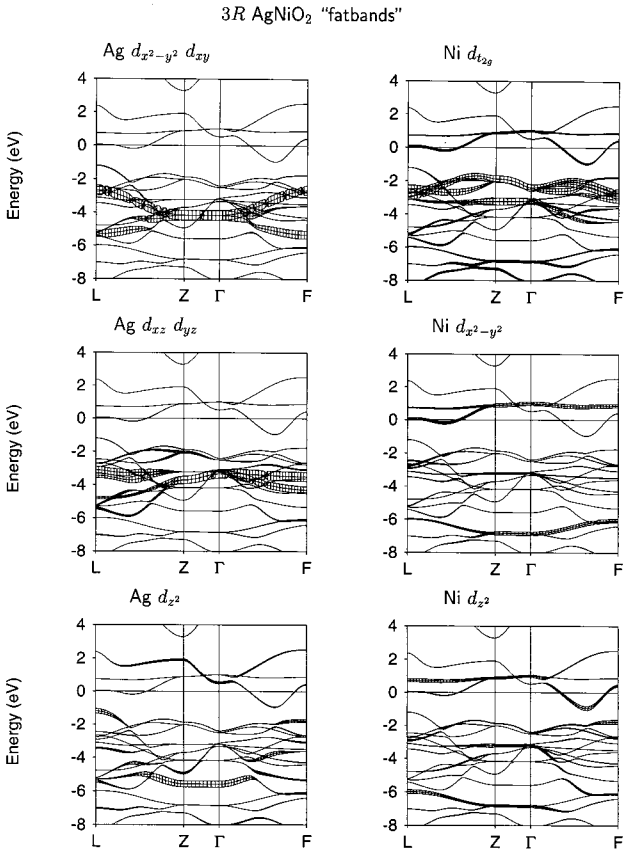

Figure 7. Selected fatbands of 3R $AgNiO_2$.

Metal e_g derived states are usually broader and therefore less susceptible to display the effects of correlation. Additionally, greater mixing with O p seen in the Ni compound would further help stabilize a metallic ground state.

The six panels of Figure 5 similarly compare the orbital-projected DOS of the 3R delafossites $PdCoO_2$ and $PtCoO_2$. In the Pd and Pt compounds, the A cations are in a d^9 configuration and make a significant contribution to the states at the Fermi energy. Comparing the DOS due to Co d in $AgCoO_2$ (Figure 3) and in $PdCoO_2$ (Figure 5), one observes minimal change, except that the Co d states in metallic $PdCoO_2$ are slightly broader. The Pd and Pt d states are also broader than the Ag d states. The fact that the DOS are not sharply peaked at E_F suggests that the systems as described by the LDA should be reliable. One interesting outcome of the comparison is that on going from Pd to Ag on the A site of the delafossite structure, one does not see the sort of nearly rigid-band behavior that we saw with respect to the d levels of the B cations in the silver delafossites.

Fatbands. The panels in the next three figures display, in the fatband representation, the band structures of the 3R delafossites $AgCoO_2$, $AgNiO_2$, and $PdCoO_2$. In all the figures, pure orbital character, a "100%" fatband, is decorated with a width of 2.5% of the total energy scale, or in this case, 0.3 eV. A point to be noted is that for the B atoms, the coordinate system has been transformed through a solid angle such that the orbitals are labeled (d_{xy}, d_{xz}, etc.) with respect to their ligands instead of the crystallographic *a* and *c* axes. For the A atoms, such reorientation is not necessary.

Following geometric considerations, we display the Ag d orbital fatbands in the manner shown in Figure 6, separating the d orbitals in the $a-b$ plane of the structure (d_{xy} and $d_{x^2-y^2}$) from those with some *z* component (d_{xz} and d_{yz}) and from d_{z^2} which, due to the crystal field of the oxygen ions proximal along the *z* axis, is most destabilized.

As expected, all the d levels of Ag are well-stabilized, being at least 2 eV below E_F. The exception is Ag d_{z^2}, which seems to make a contribution to states above E_F. This is resolved on considering the Ag s and p derived bands (not shown), which are seen to mix strongly with d states, so that a d^{10},s^0 configuration for Ag^+ is no longer valid. Considering the Co derived fatbands in Figure 6, we see a clear separation of t_{2g} and e_g states in this low-spin d^6 system. This separation defines the band gap. At the Γ point, Co $d_{x^2-y^2}$ and d_{z^2} are not separated, pointing to the octahedral squashing having no effect on the degeneracy of these levels.

The addition of one electron to the formula unit on going from 3R $AgCoO_2$ to 3R $AgNiO_2$ is demonstrated by comparing the fatbands in Figure 7 with those in Figure 6. The position on the energy axis of the Ag d_{xy}, $d_{x^2-y^2}$, and d_{yz} levels remain unchanged with respect to the Fermi level on going from $AgCoO_2$ to $AgNiO_2$. The extra electron in $AgNiO_2$ only serves to push E_F through the Ni e_g levels. The insulator−metal transition on going from $AgCoO_2$ to $AgNiO_2$ is thus explained purely from the electron count.[37]

(37) This is true for the end-members in the series 3R $AgCo_{1-x}Ni_xO_2$. The transport behavior of the alloy compositions $0 < x < 1$ will be strongly influenced by the effect of disorder on the mobility edge as pointed out by Shin et al. in ref 9.

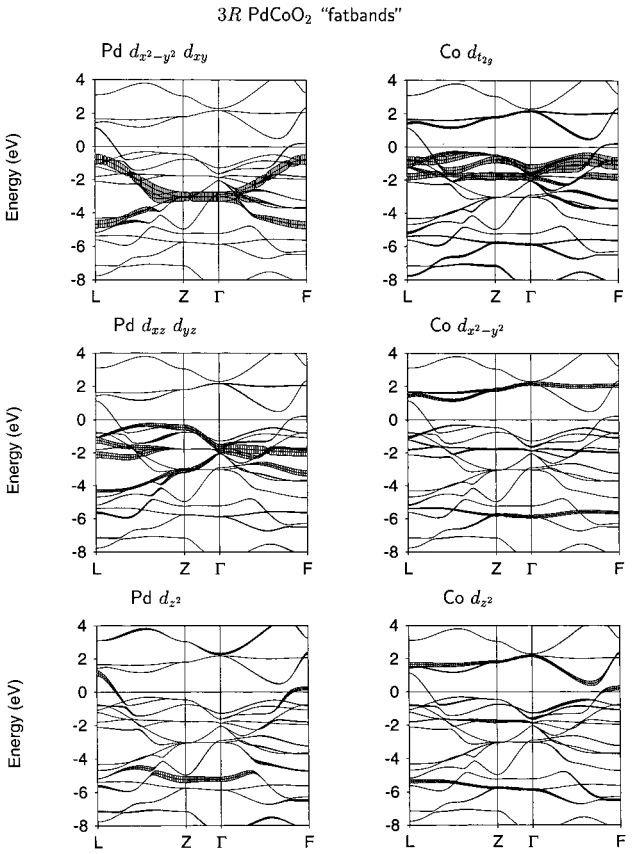

Figure 8. Selected fatbands of 3R $PdCoO_2$.

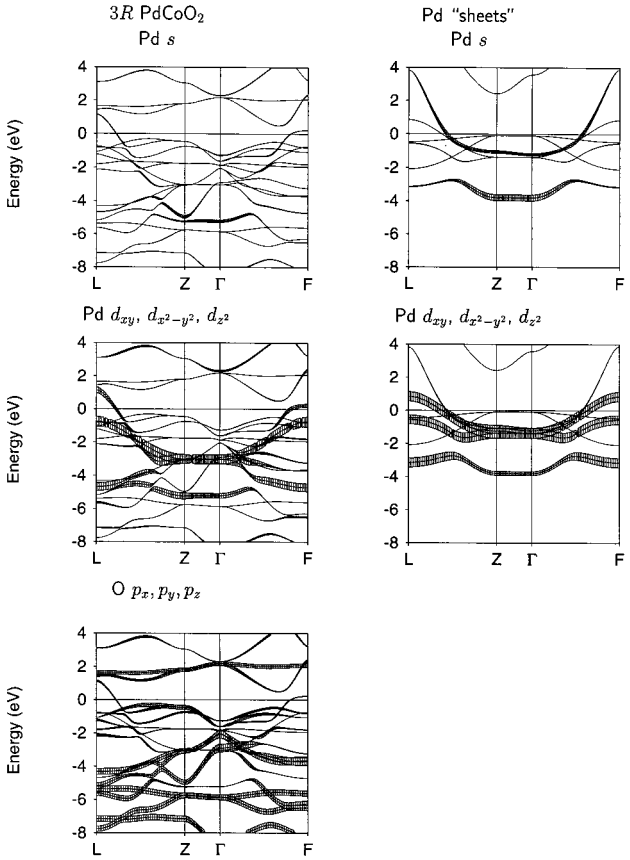

Figure 9. Selected fatbands of 3R $PdCoO_2$ and a comparison with the band structure of sheets of Pd obtained by replacing Co and O in 3R $PdCoO_2$ with empty spheres.

The six panels of Figure 8 display the metal orbital derived fatbands of 3R $PdCoO_2$. While the removal of a single d electron from the A site leaves the Co-derived fatbands of $PdCoO_2$ nearly unaffected, the Pd-derived fatbands are destabilized so that Pd d_{z^2} now crosses the Fermi energy. Due to symmetry, some small Co d_{z^2} contribution is seen crossing the Fermi energy near the *F* point of the BZ. The dominant contribution to states at E_F is from the A cation. Co remains low-spin in this compound.

Metal−metal bonding within the sheets is an interesting feature of the delafossites and, at first sight, slightly counterintuitive. Late transition metals such as Pd and Pt are expected to have more compact d orbitals than early transition metals such as Nb. Thus while metal−metal bonding is the norm with metals such as Nb, it has received less attention in Pd and Pt oxides. Of additional interest is that short Pd−Pd or Pt−Pt contacts are sustained in the delafossites, despite their being prepared under highly oxidizing conditions.

To understand the nature of the bonding and also whether it influences the rather large (of the order of 6 eV) dispersion of the d_{z^2} fatbands of the A atoms seen in Figures 6−8, we examine some more fatbands. Following the analysis of Hughbanks and co-workers[38,39] on metal−metal bonding in MoS_2 (which also has nearly close packed metal atom sheets) we consider a d^3 hybridization scheme involving linear combinations of d_{xy}, $d_{x^2-y^2}$, and d_{z^2} orbitals of the A atoms. These hybrid orbitals should result in a bonding combination that has six lobes pointing toward similar lobes on each of the six neighboring atoms in the plane. This scheme can be extended through the sheet without frustration and should result in high dispersion and strong bonding. We present in the panels of Figure 9 some more fatbands of 3R $PdCoO_2$ and those of a hypothetical sheet compound with the structure of 3R $PdCoO_2$ but with the Co and O atoms replaced by empty spheres. Following the manifold of the s fatbands in the two compounds, we see that the extra electron in the Pd "sheets" results in this manifold being raised by about 2 eV with respect to the E_F. The components of the d^3 hybrid orbitals, namely, d_{xy}, $d_{x^2-y^2}$, and d_{z^2} are also similarly raised in energy in the sheet compound. The manifold of the Pd d orbitals (especially that of Pd d_{z^2}) in the delafossite has an extra dispersion of about 2 eV. The interpretation is as follows. The change on going from the sheets to the delafossite, involves s being ionized and the Pd d_{z^2} orbital (which has the same nodal properties as s) taking on some of the character (in terms of dispersion) of the s orbital. In terms of the hydridization, going from the Pd sheet to the delafossite, the orbitals within the Pd sheets change from sd^2 to d^3. From the O p fatband in Figure 9, we particularly note that the dispersion of the Pd d_{z^2} does not arise from mixing with O p_z. It is interesting that the individual components of the d^3 hybrid orbitals are so little affected in going from the delafossite to the A atom sheets, apart from the effect of the different electron count and its influence on the position of the E_F. The reason can be linked to the fact that the crystal field of the oxygen is normal to the in-plane hybrids in the delafossite, so the perturbation is minimal. We have confirmed some of these

(38) Tian, Y.; Hughbanks, T. *Inorg. Chem.* **1993**, *32*, 400.
(39) Yee, K. A.; Hughbanks, T. *Inorg. Chem.* **1991**, *30*, 2321.

notions through an analysis of the real space electron densities (RHO) decorated with the electron localization functions (ELF) which use the extent of electron localization to demarcate regions with high bonding character. The analyses of the RHO+ELF of delafossites and other materials with hexagonal sheets of closely packed metal atoms will be presented elsewhere.

Upon examining the eigenvectors at some special points in the band structure of 3R $PdCoO_2$, the counterintuitive absence of dispersion of Pd d_{z^2} in the $Z-\Gamma$ direction is seen to stem from symmetry. The eigenvectors are mostly Pd z^2 and s in a bonding combination, in this region. At both these points, there is O p_z involvement but in a manner such that the p_z orbital from O above Pd cancels perfectly the p_z orbital from the O below. This analysis of the nature of the orbitals is to a large part valid for the other delafossites phases discussed here.

Crystal Orbital Hamiltonian Populations. The magnitude of the metal−metal bonding can be seen from Figure 10, where the COHPs due to Ag−Ag interactions in $AgCoO_2$ and $AgNiO_2$ and Pd−Pd interactions in $PdCoO_2$ are shown. The interactions have been scaled to an A−A pair. A positive COHP at a specific energy implies that the states are bonding and a negative COHP implies antibonding states. The bulk of the bonding interaction below the E_F can be compared with the corresponding *A* atom fatbands and is seen to arise largely from the dispersions of the d_{xy}, $d_{x^2-y^2}$, and d_{z^2} orbitals in all three compounds. We see that the Ag−Ag interaction at E_F is nonbonding, and as a result of this, there is almost no change in the nature of the COHP on going from $AgCoO_2$ to $AgNiO_2$. Pd states are present at E_F and are antibonding in $PdCoO_2$. An interesting feature is the presence of bonding Ag states above E_F. This is absent in the Pd−Pd interaction. The reason turns out to be the stronger mixing of d, s, and p states in the case of Ag. This effect has been remarked upon in the case of certain mixed oxides of silver and lead.[40]

It is amusing to note that metallic behavior in materials such as TiO is explained on the basis that the metal atoms are sufficiently close that there is significant overlap between the orbitals on the metal atoms. On the other hand, oxides such as ReO_3 are metallic in the absence of such direct overlap. In the case of $AgCoO_2$, there is such overlap but due to an unfavorable electron count, the system remains insulating. This is also the case in transition metal dichalcogenides such as MoS_2.[39]

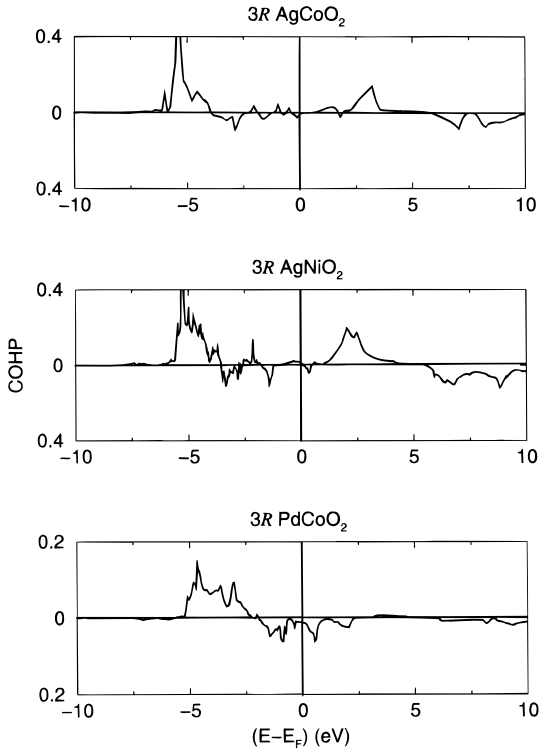

Figure 10. Crystal orbital Hamiltonian Populations considering A−A interactions in $AgCoO_2$, $AgNiO_2$, and $PdCoO_2$.

Acknowledgment. It is a pleasure to thank Professor O. K. Andersen and Dr. O. Jepsen for providing the LMTO codes and for support and encouragement. Financial support from the German Fonds der chemischen Industrie is acknowledged. We thank anonymous referees for their suggestions.

CM980079V

(40) Brennan, T. D.; Burdett, J. K. *Inorg. Chem.* **1994**, *33*, 4794.